High-Power Single-Mode Operation in DFB and FP Lasers Using Diffused Quantum-Well Structure

S. F. Yu, C. W. Lo, and E. Herbert Li, *Senior Member, IEEE*

***Abstract*—Distributed feedback (DFB) and Fabry–Perot (FP) semiconductor lasers with step and periodic interdiffusion quantum-well structures are proposed for high-power single-longitudinal-mode operation. It is shown that the phase-adjustment region formed by the diffusion step (i.e., step change in optical gain and refractive index) counteracts the influence of spatial hole burning, especially for DFB lasers with large coupling-length products biased at high injection current. Furthermore, it is found that with careful design of the diffusion grating (i.e., grating period and amount of diffusion extent) of FP lasers, side-mode suppression ratio can be enhanced and threshold current density can be minimized to a satisfied level.**

***Index Terms*—Annealing, diffusion processes, distributed feedback lasers, Fabry–Perot resonators, laser modes, quantum wells, semiconductor device modeling, semiconductor lasers.**

I. Introduction

HIGH-POWER AlGaAs–GaAs semiconductor lasers with stable single-longitudinal-mode operation are well suited for wavelength-selective applications such as frequency doubling and atomic spectroscopy [1]. Distributed feedback (DFB) lasers with $\lambda/4$ phase-shifted are effective to provide single-longitudinal-mode operation. However, stability is not maintained at high optical power especially for devices with large coupling-length products ($\kappa L > 1.25$) [2] due to nonuniform distribution of the refractive index which is a consequence of the longitudinal spatial hole burning (SHB) of carrier concentration [3]. Alternatively, new laser structures such as chirped gratings [4]–[6] or sampled gratings [7] are proposed to minimize the influence of longitudinal SHB in DFB lasers.

A simple fabrication technique and low production cost are the major advantages of Fabry–Perot (FP) lasers over other devices. However, the side-mode discrimination in an FP laser is poor especially for low-power operation or under direct electrical modulation. This is because the longitudinal-mode discrimination is mainly determined by the material gain spectrum and is not affected by cavity loss or facet reflectivity [8]. Therefore, it is necessary to improve the side-mode suppression ratio (SMSR) without sacrificing the simple fabrication procedures of FP lasers. In this paper, we investigate the possibility of using a diffused quantum-well (DFQW) structure to improve the SMSR of DFB and FP semiconductor lasers.

A diffusion step along the longitudinal direction of the active region of the quantum wells (QW's) is proposed to enhance high-power stable longitudinal-mode operation of a uniform-grating DFB laser with large κL. The operation principle of the DFQW DFB laser can be explained as follows.

1) The step DFQW's section provides a $\lambda/4$ phase-shifted for single-longitudinal-mode oscillation.
2) Because the DFQW DFB laser has a uniform grating, the longitudinal SHB is less severe than the conventional $\lambda/4$ DFB laser.
3) The step DFQW's profile compensates for any variation of refractive index arisen from longitudinal SHB of carrier concentration [2] and temperature effects [9] such that single-longitudinal-mode operation can be maintained at high power.

Therefore, significant reduction in SHB can be obtained by using a step DFQW structure.

A periodic DFQW structure is also proposed to improve the SMSR of FP semiconductor lasers. A periodic variation of refractive index and gain is created in the extent of interdiffusion along the longitudinal direction of the QW's active region which acts as a filter for the side modes. This DFQW FP laser is similar to a complex-coupled DFB laser with a high-order grating. The advantage of our proposed structure is that the complex grating can be in-phase or anti-phase; the choice depends on our selection of interdiffusion pattern and operating wavelength. However, we should avoid the following effects of DFQW grating in the design of FP lasers.

1) Higher order DFB modes can be excited by the diffusion grating provided that the grating period is much longer than the operating wavelength.
2) The optical gain of the QW's active layer (as well as the threshold current density) will reduce with the increase of diffusion extent.

Therefore, the period and extent of interdiffusion of the DFQW grating have to be determined for minimum number of DFB modes as well as threshold current density.

This paper is organized as follows. In Section II, the threshold and above threshold characteristics of DFB lasers with diffusion step structure are investigated. A self-consistent model of DFB lasers including the longitudinal variation of carrier concentration, photon density, refractive index, and temperature is utilized to calculate static and dynamic behavior of the proposed DFB laser. The electrical and optical properties of DFQW material are also described. In Section III, the threshold characteristics and design consideration of FP semiconductor lasers with periodic DFQW structure are presented. Finally, a brief discussion and conclusion are given in Section IV.

Manuscript received August 26, 1996; revised January 20, 1997.

The authors are with the Department of Electrical and Electronic Engineering, University of Hong Kong, Pokfulam Road, Hong Kong.

Publisher Item Identifier S 0018-9197(97)03803-7.

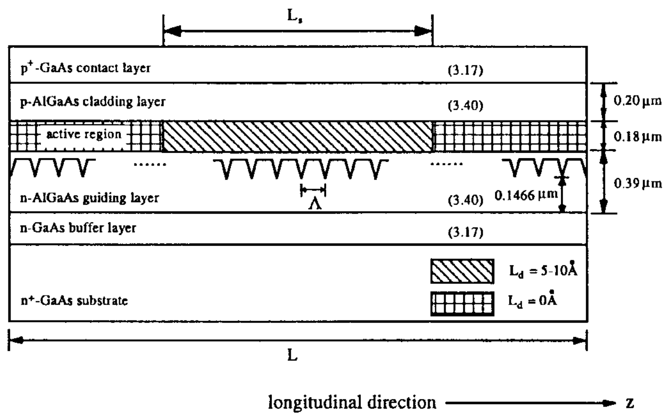

Fig. 1. Schematic of the DFB laser with diffusion step profile. L_s is the length of the diffusion step and L_d is the diffusion length.

II. Proposed DFB Lasers with Diffusion Step Profile

A. Laser Structure

The schematic diagram of a DFB laser with diffusion step is shown in Fig. 1. The laser is composed of six layers: n^+-GaAs substrate, n-GaAs buffer layer, n-AlGaAs guiding layer in which the grating is defined, followed by a QW active layer, and finally the p-AlGaAs ($\cong$0.2 μm) and p^+-GaAs ($\leq$0.3 μm) layers which form the cladder and contact, respectively. The active layer is regrown on top of the guiding layer which consists of four $Al_{0.3}Ga_{0.7}As$–GaAs single QW's with well and barrier thicknesses of 100 and 280 Å, respectively. It is proposed that a diffusion step is introduced in the center of the active region to form a phase-adjustment region (PAR) such that the optical gain and refractive index are slightly less than the as-grown region. In order to obtain a $\lambda/4$ phase-shifted, the products of propagation coefficient difference and effective length of the PAR must be equal to $\pm(\frac{1}{2}+n)\pi$, where n is a positive integer [2], [10]. The advantage of using an interdiffusion technique to form a PAR over 1) a phase-adjusted waveguide [2], [10] or 2) corrugation-pitch modulation [3] is that only simple fabrication procedures are required (i.e., DFQW structure can be easily obtained by impurities implantation and thermal annealing).

B. Models for DFB Lasers and QW Material

The propagation of forward and reverse fields, F and R, along the laser cavity can be described by the time-dependent coupled optical wave equations given as follows [11]:

$$\left(\frac{1}{\nu_g}\frac{\partial}{\partial t} \pm \frac{\partial}{\partial z}\right)\begin{bmatrix}F\\R\end{bmatrix} = \left[\frac{1}{2}(\Gamma G - \alpha_s) + j\delta\beta\right]\begin{bmatrix}F\\R\end{bmatrix} + j\kappa\begin{bmatrix}R\\F\end{bmatrix} + \begin{bmatrix}j_{Fs}\\j_{Rs}\end{bmatrix} \quad (1)$$

where $j=\sqrt{-1}$, κ is the coupling coefficient, G is the modal gain, α_s is the absorption and scattering loss of the QW waveguide, $j_{Fs,\,Rs}$ is the spontaneous emission, ν_g ($= c/n_g$, where n_g is group index and c is the velocity of light in free space) is the group velocity, and Γ is the transverse optical confinement factor. The deviation from Bragg's condition, $\delta\beta$, is given as

$$\delta\beta = \frac{\omega_o}{c}(ne + \Delta n\Gamma) - \frac{\pi}{\Lambda} \quad (2)$$

where $\omega_o(= 2\pi c/\lambda_o)$ is the lasing frequency, λ_o is the operating wavelength, and Λ is the period of grating. ne is the effective refractive index of the grating waveguide and Δn is the change of refractive index due to the variation of carrier concentration. ne can be evaluated by the effective index method provided that the refractive index profile of the laser is known. The time-dependent rate equation of carrier concentration along the longitudinal direction of the active region is described by

$$\frac{\partial N}{\partial t} = \frac{J}{qN_W L_z} - \frac{N}{\tau_N} - \nu_g G P \quad (3)$$

where J is the current density, N_w is the number of QW's, L_z is the thickness of the QW, q is the electron charge, $P(= |F|^2 + |R|^2)$ is the photon density, and τ_N is the carrier lifetime. In the model, the heat distribution along the longitudinal active region is also taken into account by solving the time-dependent quasi-two-dimensional heat equation (see Appendix A). As a result, threshold and above-threshold behavior of DFB semiconductor lasers with DFQW structure can be obtained by solving (1), (3), and the heat equation in a self-consistent manner [11].

The refractive index and optical gain of QW material under the influence of impurities-induced compositional disordering are also considered in our analysis. The models given in [12]–[14] are utilized to calculate the optical and electrical properties of DFQW's which are summarized in Appendix B. It is defined that the extent of diffusion into the QW material is characterized by a diffusion length, $L_d[=\sqrt{(D\tau_a)}]$ where τ_a is the annealing time and D is the temperature-dependent diffusion coefficient [15]. It is assumed that $L_d = 0$ Å represents the as-grown QW's and the diffusion extent is described by the magnitude of L_d. Fig. 2 shows the influence of L_d on the optical gain and refractive index spectrum (TE polarization) of the QW material (at 300 K). It is observed, for $\lambda_o \geq 0.85$ μm, the optical gain as well as the refractive index are reduced with L_d. In the following calculations, it is assumed that the lasers have perfect antireflection coating on both facets. Furthermore, the parameters used in the calculation are given in Tables I–III.

C. Threshold Characteristics of Diffusion-Step DFB lasers

Fig. 3 shows the gain margin and the detuned wavelength of the gap mode [16] $\delta\lambda(= -\delta\beta\lambda_o^2/2\pi n_g)$ against the effective length L_s of PAR for L_d equal to 5 and 10 Å. It is assumed that κL varies between 1.25 and 2.8. For a device with $L_d =$ 5 Å [see Fig. 3(a)], it is observed that the gain margin has a peak for L_s varies between 120 and 160 μm. The wavelength of the gap mode decreases monotonically with L_s due to the reduction of effective refractive index along the cavity. For $L_d = 10$ Å [see Fig. 3(b)], the devices exhibit similar characteristics to $L_d = 5$ Å. However, the range of L_s for peak gain margin is reduced with the increase of L_d due to the reduction of refractive index and optical gain inside the PAR. It must be noted that the peak gain margin of the conventional

TABLE I
PARAMETERS USED IN THE MODEL

Parameters (symbol)	Magnitude
Operating wavelength (λ_o)	0.85 μm
Grating Period (Λ)	0.127 μm
Absorption and scattering loss in waveguide (α_s)	40 cm^{-1}
Width of active layer (w)	2.0 μm
Total thickness of active layer (t_d)	0.18 μm
Thickness of the quantum well (L_z)	100 Å
Number of quantum well (N_w)	4
Carrier lifetime (τ_N)	3 ns
Effective group refractive index (n_g)	3.70
Length of laser cavity (L)	400 μm
Velocity of light in free space (c)	3×10^{10} cms^{-1}

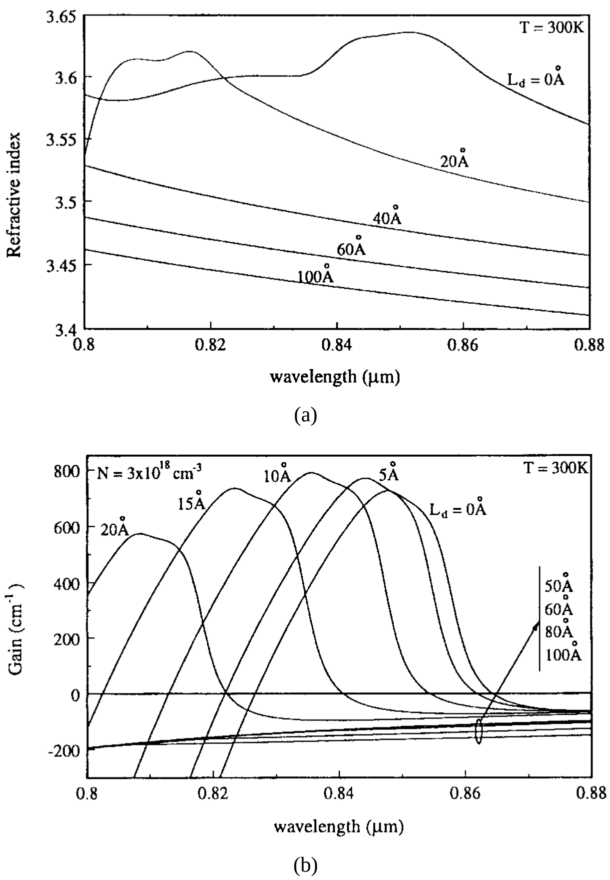

Fig. 2. Calculated (a) background refractive index and (b) optical gain spectra of $Al_{0.3}Ga_{0.7}As$–GaAs QW at carrier concentration, $N = 3 \times 10^{18}$ cm^{-3} with various levels of L_d.

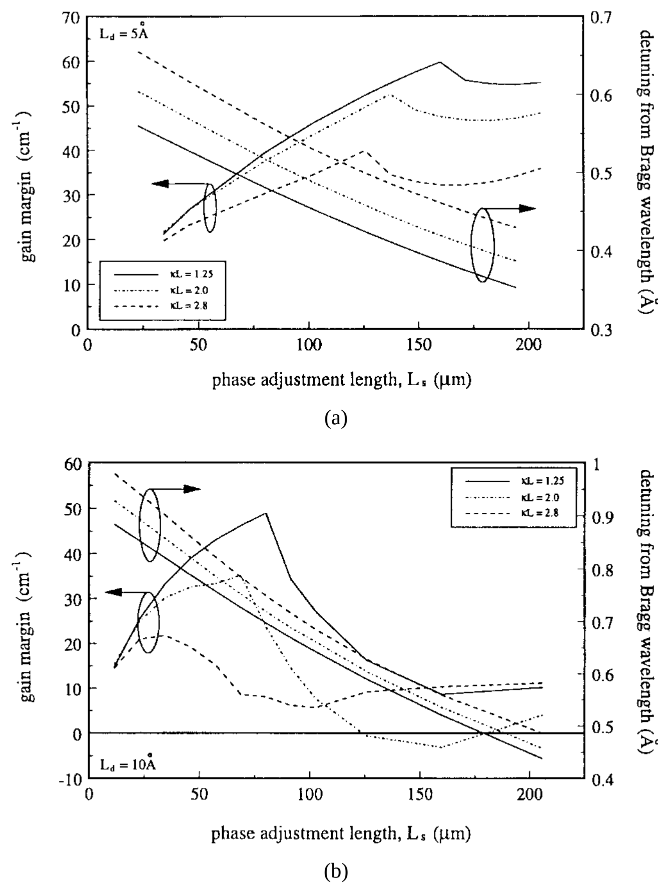

Fig. 3. The variation of gain margin and detuning wavelength of gap mode against L_s for devices with κL = 1.25, 2.0, and 2.8. It is assumed that (a) L_d = 5 Å and (b) L_d = 10 Å.

phase-adjusted waveguide devices [2], [10] is independent of the length of PAR.

D. Static and Dynamic Characteristics of Diffusion-Step DFB Lasers

Fig. 4 compares the variation of SMSR with normalized injected current density, J/J_{th} (where J_{th} is the threshold current density) at steady state for the lasers with (L_d = 5 Å) and without (conventional discrete $\lambda/4$ DFB laser) step diffusion profile. Multimode operation (defined by a drop of SMSR from 50 to 10 = 40 dB) is observed for conventional $\lambda/4$ DFB laser with $\kappa L \geq 3.2$. However, stable single longitudinal mode is maintained for laser with step diffusion profile. This is because of the built-in step refractive index profile against the carrier-induced index change inside the active region. The maximum output power of the lasers is larger than 50 mW at $J/J_{\text{th}} = 10$. For the device with (L_d = 10 Å), similar behavior is observed and hence it is not described again.

The relative effective refractive index profiles of devices with $\kappa L = 3.2$ and biased at $J = 9J_{\text{th}}$ are shown in Fig. 5. As we can see, the conventional $\lambda/4$ DFB laser exhibits nonuniform (concave-up) distribution of refractive index with peak to peak value, Δn_p, equal to 0.0015. However, the

TABLE II
MATERIAL PARAMETERS IN THE LASER STRUCTURE

(at operating wavelength of 0.85μm)	Diffusion Length (L_d) 0 Å	5Å	10Å	20Å
Fitted parameter (a_o) cm^{-1}	1591.6434	1384.6995	432.1735	65.5869
Transparency carrier density (N_o)x10^{18} cm^{-3}	1.9399	1.8587	2.2196	11.7549
Fitted parameter (d_o)	-0.02830	-0.02783	-0.02644	-0.02539
Fitted parameter (N_r)x10^{18} cm^{-3}	2.0557	1.9771	2.4109	11.7883
Refractive index (n_r)	3.6270	3.6074	3.5880	3.5360
Effective refractive index (ne)	3.302938	3.301600	3.300346	3.296800

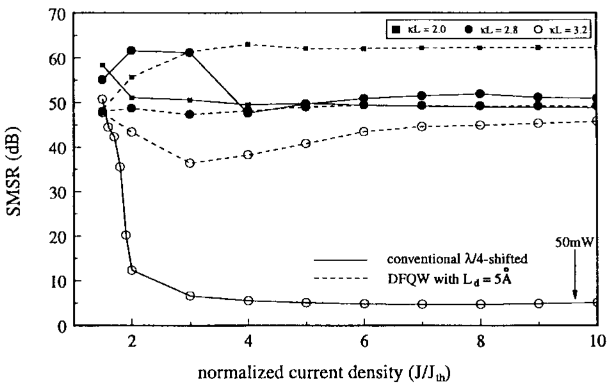

Fig. 4. The SMSR various with normalized current, $J/J_{\rm th}$, for lasers with $\kappa L = 2.0$ (■), $\kappa L = 2.8$ (•), and $\kappa L = 3.2$(○). The solid and dash lines represent the cases for the conventional $\lambda/4$ phase-shifted DFB laser and step-diffused device ($L_d = 5$ Å).

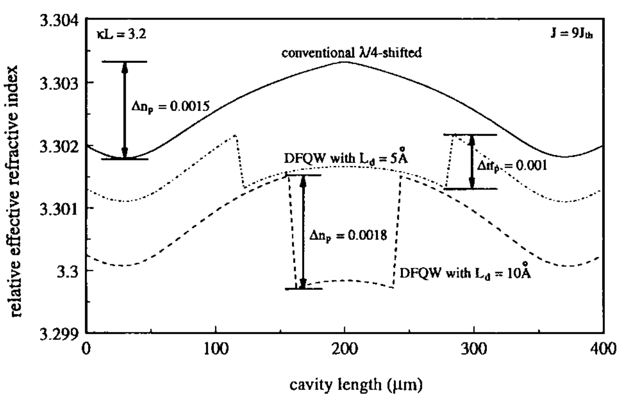

Fig. 5. Longitudinal refractive index profile of the conventional $\lambda/4$ DFB laser (solid line), DFQW laser with $L_d = 5$Å (dashed–dotted line) and DFQW laser with $L_d = 10$ Å (dashed line). The devices are biased at $J = 9J_{\rm th}$ with κL equal to 3.2.

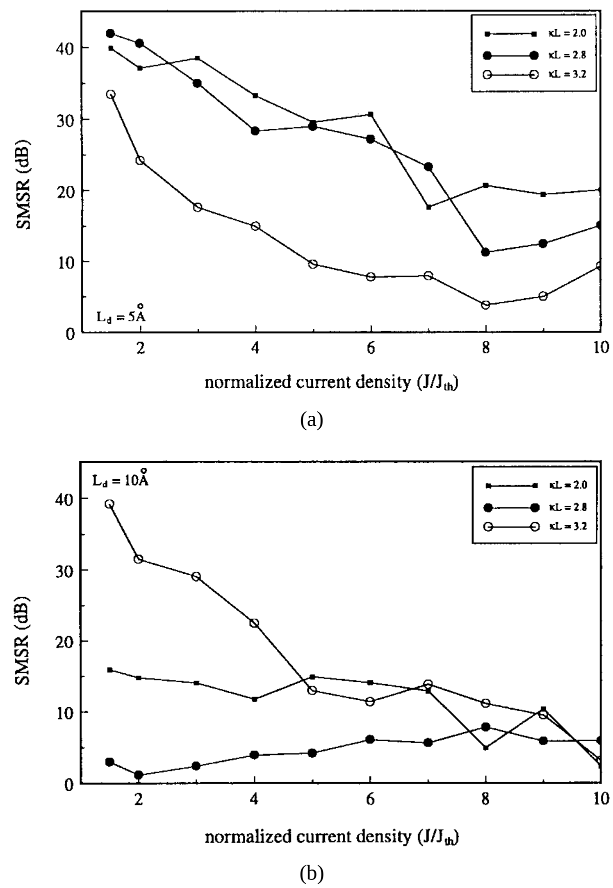

Fig. 6. The SMSR of the first overshoot power spectrum various with normalized current, $J/J_{\rm th}$, for a device with diffusion length (a) $L_d = 5$ Å and (b) $L_d = 10$ Å. The symbols (■), (•), and (○) represent $\kappa L = 2.0$, 2.8, and 3.2, respectively.

uniformity of the effective refractive index is maintained for $L_d = 5$ Å with $\Delta n_p = 0.001$. For $L_d = 10$ Å, the built-in refractive index step is larger than the required to overcome the SHB effects and Δn_p is found to be equal to 0.0018. Therefore, only a small range of L_d (5 Å $\leq L_d <$ 10 Å) will satisfy the requirement to minimize the influence of SHB effects. It must be noted that device with $L_d < 5$ Å is not realistic due to the limitation of controlled interdiffusion.

The spectrum purity of the turn-on transient signal determines the maximum modulation bandwidth of the lasers. In our purposed DFB lasers, a built-in step refractive index profile is introduced (by interdiffusion) which may affect the spectrum purity of the lasers as SHB is negligible during the turn-on time interval. Fig. 6 shows the influence of built-in index step on the SMSR at the first overshoot of lasers with $L_d = 5$ and 10 Å. As we can see, SMSR is reduced with the increase of injection current and devices with low κL exhibit better SMSR. The reduction of SMSR can be attributed to the built-in index profile because no SHB is taken place during the first overshoot of the output power. The built-in refractive index step reduces the gain requirement of the band-edge mode. Therefore, excitation of band-edge mode is observed in both cases and the case $L_d = 10$ Å is more pronounced than $L_d =$ 5 Å.

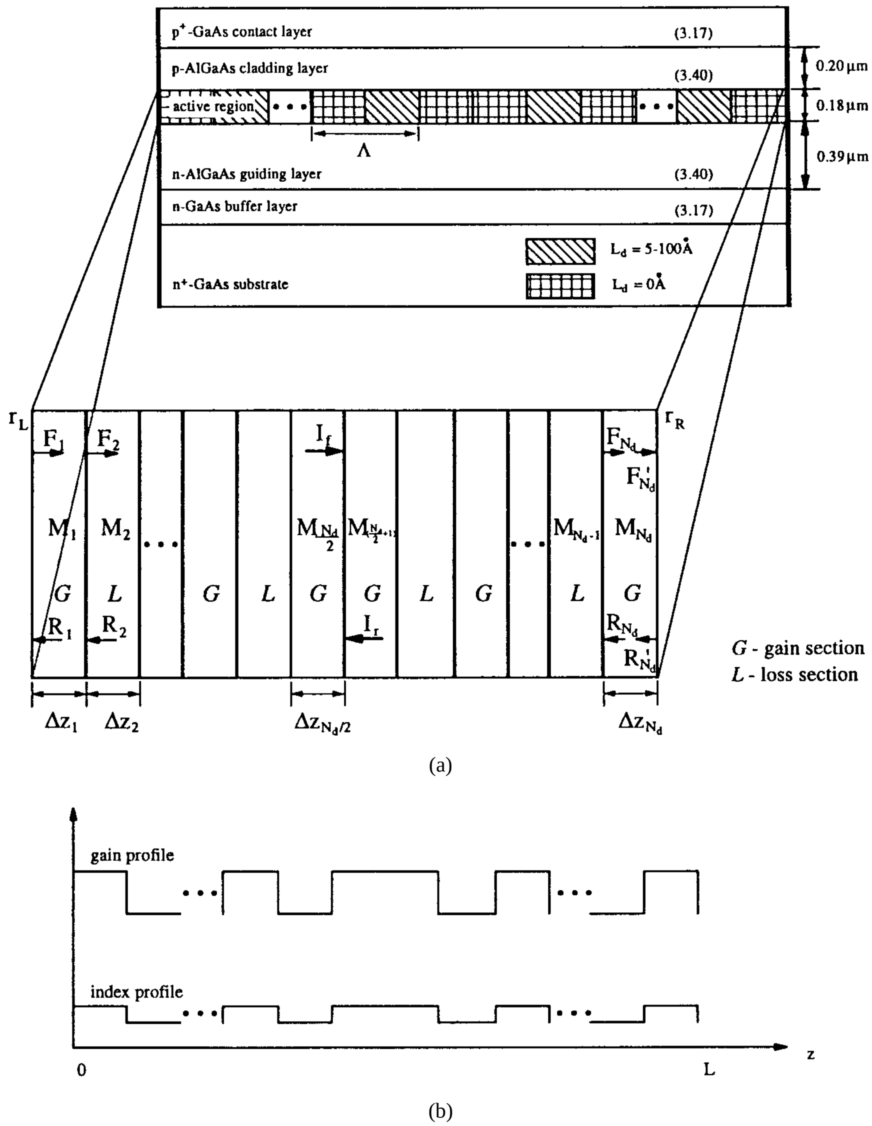

Fig. 7. (a) The schematic of an FP laser with periodic DFQW structure. (b) The periodic variation of gain and built-in refractive index profile along the QW active region is due to the periodic change of diffusion length.

III. Proposed FP Lasers with Periodic DFQW Structure

A. Laser Structure

Fig. 7 shows the schematic diagram of a FP laser with periodic DFQW structure. The device is similar to that given in Fig. 1 except no grating is introduced. The periodic variation of gain and refractive index (along the longitudinal direction of active region) is obtained by periodic interdiffusion. The as-grown QW section ($L_d = 0$ Å) serves as gain region while the diffused section ($L_d = 5$–100 Å) serves as the loss region with large differences of refractive index as well as optical gain. The longitudinal length of each diffused section, Δz_k (for $k = 1, 2, \cdots, N_d$), is equal to a multiple of $\lambda_o/4$, where N_d is the total number of diffused sections. The device's total length is set to 400 μm with N_d varying between 8 and 160, which can be done by alternating the period of the diffusion grating. The left and right facet reflectivities of the laser cavity are both assumed to be 0.55.

B. Model for FP Lasers with Periodic DFQW Structure

The optical fields propagating along the diffusion grating can be calculated by using the transfer matrix method [17]. In each diffused section, carrier density, photon density, refractive index, and other material parameters are assumed to be constants but all these parameters can be varied along the cavity. The spontaneous emission can also be taken into consideration by introducing between sections [18]. Detailed modeling of optical fields inside the active region can be found in Appendix C. The rate equation of carrier concentration along the DFQW's active region is described by

$$\frac{dN_k}{dt} = \frac{J}{qN_wL_z} - \frac{N_k}{\tau_N} - \nu_g \sum_m \Gamma_k G_k(\lambda_m) P_k(\lambda_m) \tag{4}$$

where k is the section number, λ_m is the mode wavelength, P_k is the photon density, and Γ_k is the transverse optical confinement factor of the kth section. The below and above

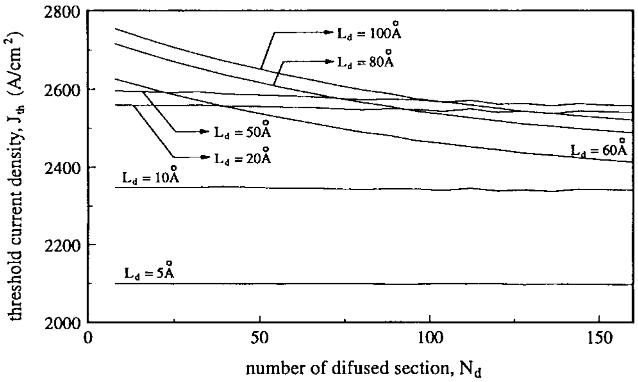

Fig. 8. The threshold current density against total number of diffused sections with the gain region is defined by diffusion length, $L_d = 0$ Å, and L_d in the loss region is set to 5, 10, 20, 50, 60, 80, and 100 Å, respectively.

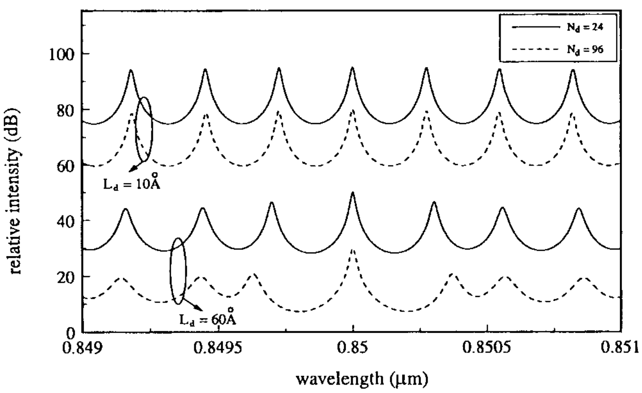

Fig. 9. Threshold emission spectra of DFQW's FP lasers for $L_d = 10$ Å and $N_d = 24$, $L_d = 10$ Å and $N_d = 96$, $L_d = 60$ Å and $N_d = 24$, and $L_d = 60$ Å and $N_d = 96$.

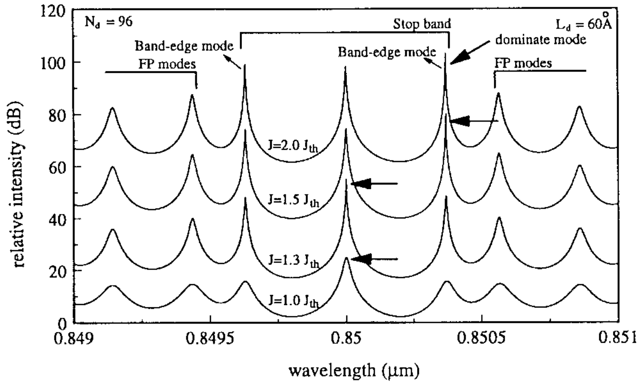

(a)

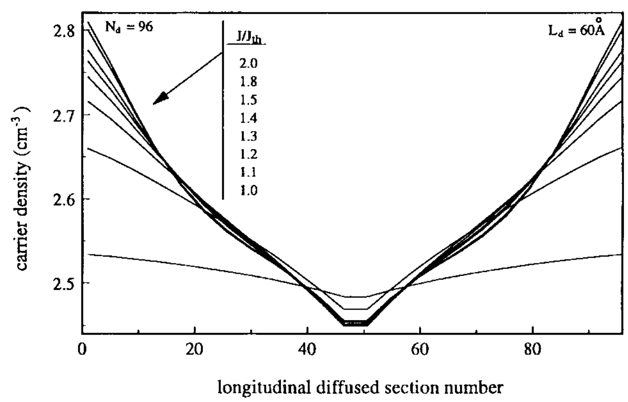

(b)

Fig. 10. (a) The spontaneous emission power spectra of DFQW FP lasers. The device has 96 gain/loss diffused sections and L_d's combination is equal to 0|60 Å. The injection current density is set to $1.0J_{\rm th}$, $1.3J_{\rm th}$, $1.5J_{\rm th}$, and $2.0J_{\rm th}$. (b) The carrier concentration profile of the lasers with injection current density set to $1.0J_{\rm th}$, $1.1J_{\rm th}$, $1.2J_{\rm th}$, $1.3J_{\rm th}$, $1.4J_{\rm th}$, $1.5J_{\rm th}$, $1.8J_{\rm th}$, and $2.0J_{\rm th}$.

threshold optical spectral can be obtained by solving the transfer matrix equation, carrier rate equation, and heat equation self-consistently.

C. Below and Above Threshold Characteristics of DFQW FP Lasers

Fig. 8 shows a plot of the threshold current density, $J_{\rm th}$, of the periodic DFQW's FP laser against the total number of diffused sections, N_d, with L_d as a variable parameter. It is found that for large L_d (>50 Å), $J_{\rm th}$ is inversely proportional to N_d. In addition, a maximum $J_{\rm th}$ is located at L_d's combination approximately equal to 0|100 Å for $N_d < 80$ and equal to 0|50 Å for $N_d > 80$. This is because the optical distributed feedback is affected by the design of the periodic DFQW structure. It is noted that optical gain at 0.85 μm can only be obtained by external carrier injection for DFQW's with $L_d < 15$ Å [see Fig. 2(b)]. For $L_d > 60$ Å, optical feedback is enhanced due to the large difference in gain and refractive index between grating sections (see Fig. 2). Therefore, low threshold current density can be obtained at $L_d < 10$ Å or $L_d > 60$ Å and is also a function of N_d. It must be noted that the threshold current density of FP lasers without periodic DFQW structure is equal to 2123 A/cm^2. Fig. 9 shows the corresponding threshold-amplified spontaneous spectra for L_d's combination is equal to 0|10 and 0|60 Å (with N_d equal to 24 and 96, respectively). As shown in the figure, the bandgap mode is dominant in the spectra especially for L_d's combination equal to 0|60 Å and $N_d = 96$. This is expected as the filtering properties of the periodic DFQW structure are more efficient for large magnitude of L_d and N_d. In the design of devices with DFQW's, the value of L_d should not be greater than 100 Å; otherwise the electrical and optical properties of QW's will be removed.

Fig. 10(a) shows the amplified spontaneous spectra for device with L_d's combination equal to 0|60 Å and $N_d = 96$. As we can see, when the current density increases from $1.0J_{\rm th}$ to $1.3J_{\rm th}$, the bandgap mode dominates over other longitudinal modes. Further increase in current density excites the band-edge mode (with longer wavelength) due to the SHB effects. Fig. 10(b) shows the corresponding longitudinal distribution of carrier concentration at different injection levels. At the injection level equal to $1.5J_{\rm th}$, the longitudinal carrier distribution changes rapidly due to the excitation of band-edge mode but it is stabilized with further increase in injection current.

As we have mentioned before, because the period of the diffusion grating is in the order of 5 μm, it is expected that the DFB modes are repeated in the optical spectrum. In order to avoid the influence of the high-order DFB modes, the bandgap mode should be selected in coherent with the optical gain peak of the active region ($L_d = 0$ Å) such that other DFB modes away from the peak gain wavelength are suppressed. In the above calculations, it is assumed that the wavelength of the bandgap mode (i.e., $\lambda_o = 0.85$ μm) is coherent with the optical gain peak (QW's active region with $L_d = 0$ Å).

IV. Discussion

The success of our proposal depends upon whether we can realize the DFQW semiconductor lasers in practice using existing fabrication technologies such that the production cost and waste in the device's fabrication can be further reduced. The following must be noted.

1) The proposed semiconductor lasers have typical dimensions which require a simple processing technique and are compatible with existing fabrication technologies.
2) Interdiffusion of QW's requires the penetration of impurities or vacancies through the contact and cladding layers into the active region such that the contact and cladding layers form a blocking layer of the diffusion process. However, the total thickness of the p^+-GaAs contact layer and the p-AlGaAs cladding layer is less than 1 μm, which allows the diffusion process to be carried out [19].
3) The diffusion length L_d of DFQW's active region is determined by the implantation energy and thermal annealing time of the interdiffusion process. With careful control of annealing temperature and time, L_d down to 5 Å can be obtained without any difficulty.
4) The formation accuracy of DFQW's grating determines the yield rate of single-longitudinal-mode operation of the FP lasers. The combined technologies of electron beam lithography and implantation-enhanced intermixing [20] are utilized to realize a structure which is far more precise than the required micron DFQW grating.

In fact, the use of DFQW's structure to improve single-longitudinal-mode operation of $\lambda/4$ DFB lasers has been proposed [21] and gain-coupled DFB lasers with periodic DFQW structure have also been fabricated [22]. These indicated that our proposed DFQW structures can easily be realized in practice. The other advantages for adopting DFQW structure are: 1) tunability of the operating wavelength by modifying the diffusion profile; 2) the use of the interdiffusion technique to form a PAR in DFB lasers can avoid the complex fabrication process in $\lambda/4$ phase-shifted corrugation; and 3) enhanced yield rate of single-longitudinal-mode operation of uniform grating DFB lasers and FP lasers.

V. Conclusion

We have proposed novel structures for DFB and FP semiconductor lasers by interdiffusion of a QW active region. It is shown that stable single-longitudinal-mode operation can be maintained in DFB lasers with uniform grating at high output power. For DFB lasers with large κL, the influence of SHB at steady state can be minimized (i.e., enhancement of SMSR) with diffusion step of $L_d \geq 5$ Å and $L_d < 10$ Å. However, it is shown that SMSR is deteriorated by the diffusion step

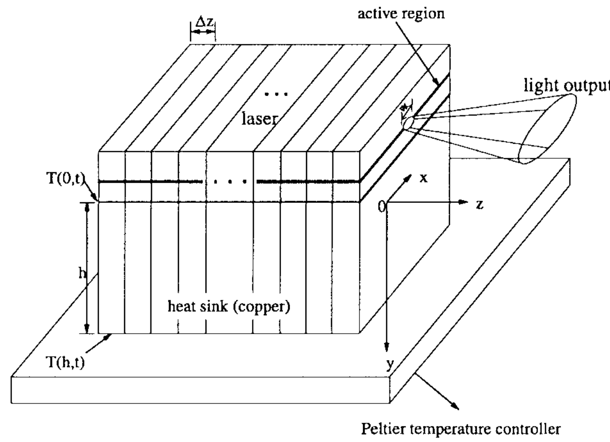

Fig. 11. Laser-mounting structure with a copper heat sink.

structure during the turn-on time interval especially for $L_d > 5$ Å. Single-longitudinal-mode operation is also achieved in DFQW FP lasers at and above threshold. It is shown that the DFQW structure also enhances the SMSR of FP lasers. This is because of the filtering effects arise from the difference of refractive index and optical gain between the diffused sections. It is revealed that a device with L_d's combination equal to 0|60 Å exhibits better spectrum purity than a device with L_d's combination equal to 0|10 Å; even the threshold current densities of both devices are close together. This is because the periodic DFQW structure demonstrates better optical filtering efficiency with large L_d which compensates for the increase of optical loss arisen from the interdiffusion effects. Although the threshold current density of the proposed FP lasers with DFQW's structure is deteriorated by 16% (compares with FP lasers without interdiffusion structure), the SMSR is enhanced by more than 10 dB at threshold.

Appendix A

In order to estimate the heat distribution along the active region, several assumptions are made.

1) The longitudinal heat distribution is analyzed by dividing the laser cavity/copper heat sink into small segments (see Fig. 11).
2) In each segment, the transverse heat flow is described by the one-dimensional time-dependent Poisson equation [23]
$$\kappa_p \frac{\partial^2 T(y,\, t)}{\partial y^2} = \rho C_p \frac{\partial T(y,\, t)}{\partial t} \tag{A1}$$
where T is the temperature measured in Kelvin, ρ is the density, C_p is its specific heat, and κ_p is its thermal conductivity of the heat sink. $y > 0$ corresponds to the copper of heat sink and $y < 0$ to all semiconductor layers.
3) Although the heat distribution is much pronounced in the lateral direction (xy plane), we ignore the influence of thermal effects along the lateral direction. This is because we concentrate on the analysis of longitudinal modes operation. Therefore, we assume the fundamental lateral mode is maintained at a high power such that the term $\partial^2 T/\partial x^2$ is ignored in (A1). Furthermore, the

lateral dimension of the laser and copper heat sink are assumed identical in order to reduce our computational effort.

4) The longitudinal thermal diffusion length is assumed to be much less than the segment length such that the longitudinal term $\partial^2 T/\partial z^2$ can be ignored in (A1).
5) The corresponding boundary conditions of (A1) are given by

$$T(h, t) = T_p$$

and

$$T(0, t) = H(t)\frac{wd}{4\kappa_p} \tag{A2}$$

where w is the width, d is the thickness of the active region, h is the height of the heat sink, and T_p is the temperature of electrical Peltier temperature controller. $H(t)$ is the power dissipated along the active region and can be approximated by

$$H(t) = \frac{N_w V_d(N) J}{L_z} - \frac{\nu_g \hbar\omega P}{\Delta z} \tag{A3}$$

where V_d is the junction voltage, N_w is the number of quantum wells, L_z is the width of wells, and N is the carrier concentration inside the active region. V_d can be approximated by [24]

$$V_d(N) = \frac{1}{q}\Bigg(E_g + k_B T \cdot \ln\left\{\left[\exp\left(\frac{N}{N_c}\right) - 1\right]\left[\exp\left(\frac{N}{N_V}\right) - 1\right]\right\}\Bigg) \tag{A4}$$

where E_g is the energy gap between the first quantized energy level of conduction and valence bands of the QW, k_B is the Boltzmann constant, and T is the temperature in Kelvin. N_C and N_V are the effective conduction and valence edge density of states, respectively. They can be expressed as $N_{c/V} = m^*_{e/h} k_B T/\pi\hbar^2 L_z$ where $m^*_{e/h}$ is the effective mass of the electron/hole.

6) The time variation of temperature can be approximated by

$$\left.\frac{\partial T}{\partial t}\right|_{y_j} \Delta t = T(y_j, t + \Delta t) - T(y_j, t) \tag{A5}$$

where j is an integer, Δt is identical to that given in the wave equations, and the time variation of the temperature is synchronized with the traveling waves and carrier concentration. Substituting (A5) into (A1), the rate equation of temperature can be written as

$$T(y_j, t + \Delta t) - T(y_j, t) = \frac{1}{\rho C_p}\left\{\kappa_p \left.\frac{\partial^2 T(y, t)}{\partial y^2}\right|_{y_j}\right\}\Delta t \tag{A6}$$

where

$$\left.\frac{\partial^2 T(y, t)}{\partial y^2}\right|_{y_j} = \frac{T(y_{j+1}, t) - 2T(y_j, t) + T(y_{j-1}, t)}{\Delta y^2} \tag{A7}$$

for y_i away for the facets of device. At the boundaries, the corresponding second derivative takes the form

$$\left.\frac{\partial^2 T(y, t)}{\partial y^2}\right|_{y_1} = \frac{2\left[T(y_2, t) - \dfrac{H(t)dw}{2\sigma}\right]}{\Delta y^2} \tag{A8}$$

$$\left.\frac{\partial^2 T(y, t)}{\partial y^2}\right|_{y_n} = -\frac{2[T_p - T(y_{n-1}, t)]}{\Delta y^2} \tag{A9}$$

where n is the total number of section, $y_1 = 0$, and $y_n = h$. In the calculation, it is assumed that $\kappa_p = 4$ W·m^{-1}·K^{-1}, $E_g = 1.519$–$5.408 \times 10^{-4} \times T^2/(T+204)$ eV, $h = 1$ mm, and $T_p = 300$ K.

APPENDIX B

The refractive index, n_{DFQW}, of the DFQW's active layer is given by [12]

$$n_{\mathrm{DFQW}}(\omega) = (\tfrac{1}{2}\varepsilon_1^T(\omega) + \tfrac{1}{2}\{[\varepsilon_1^T(\omega)]^2 + [\varepsilon_2^\Gamma(\omega)]^2\}^{1/2})^{1/2} \tag{B1}$$

where ω is the angular frequency, $\varepsilon_1^T(\omega)[= \varepsilon_1^\Gamma(\omega) + \varepsilon_1^{X,L}(\omega)]$ is the real part of the total dielectric function, and $\varepsilon_2^\Gamma(\omega)[= \varepsilon_2^{exc}(\omega) + \varepsilon_2^{bound}(\omega) + \varepsilon_2^{con}(\omega)]$ is the imaginary part of the dielectric function for the Γ valley.

The real part of the dielectric function, $\varepsilon_1^\Gamma(\omega)$, for the Γ valley is given by [12]

$$\varepsilon_1^\Gamma(\omega) = 1 + \frac{1}{\pi}\int_0^\infty \frac{\varepsilon_2^\Gamma(\omega')}{\omega' + \omega}\,d\omega' + \frac{1}{\pi}\sum_{m=1}^{M}\int_{\omega'_m}^{\omega'_{m+1}} \frac{\varepsilon_2^\Gamma(\omega')}{\omega' - \omega}\,d\omega', \qquad \omega'_m \neq \omega. \tag{B2}$$

The imaginary part of the dielectric function for the Γ valley, $\varepsilon_2^\Gamma(\omega)$, is obtained by summing over all the above contributions as follows:

$$\varepsilon_2^\Gamma(\omega) = \varepsilon_2^{\mathrm{exc}}(\omega) + \varepsilon_2^{\mathrm{bound}}(\omega) + \varepsilon_2^{\mathrm{con}}(\omega) \tag{B3}$$

where $\varepsilon_2^{\mathrm{exc}}(\omega)$ is the 1S exciton contribution derived by the density-matrix approach at the subband edge without the influence of band mixing and $\varepsilon_2^{\mathrm{bound}}(\omega)$ is the conduction-valence band bound-state contribution without the electron-hole interaction. $\varepsilon_2^{\mathrm{con}}(\omega)$ is the contribution from the unbound continuum states above the barrier, which are determined using a wider (2000-Å width) square QW above the DFQW and by the same method for the bound states.

Using the density matrix approach, the optical gain with the photon generated in the direction perpendicular to the surface of QW layers is given as [14]

$$G(\omega) = \frac{e^2 M_b^2}{\pi c\varepsilon m_o^2 \omega L_z}\sum_{p,q}\int |\langle\psi_{Cp}|\psi_{Vq}\rangle|^2 \mathbf{P}_{pq}(k) \cdot \mathbf{L}[E_p(k) - E_q(k) - \hbar\omega] \cdot \{f^C[E_p(k)] - f^V[E_q(k)]\}\,dk \tag{B4}$$

where m_o is the rest mass of electron and M_b is the optical matrix. E_p and E_q are the pth-electron and qth-hole subband-edge energy, respectively, and ψ_C and ψ_V are the envelope

TABLE III
MATERIAL PARAMETERS IN THE LASER STRUCTURE

(at operating wavelength of 0.85μm)	Diffusion Length (L_d)			
	50 Å	60Å	80Å	100Å
Fitted parameter (a_g)x10^{-18} cm^{-1}	4.3819	4.1967	7.0395	7.1861
Fitted parameter (N_g)x10^{18} cm^{-3}	29.8423	32.3840	27.3708	29.6957
Refractive index (n_r)	3.4750	3.4690	3.4590	3.4280
Effective refractive index (ne)	3.290989	3.193064	3.181995	3.178748

wavefunctions for the electrons and holes, respectively. $\mathbf{L}$ is the Lorentzian broadening factor with HWHM of 5 meV and k is the wavevector. The summation in (B4) is over all the conduction and valence subbands and $\mathbf{P}(k)$ is the TE-polarization factor. f^C and f^V are the quasi-Fermi for the electrons in the conduction and valance bands, respectively.

Using (B4), the TE optical gain, G, at 0.85 μm with L_d varying between 0 and 20 Å is approximated by

$$G = a_o(1 + a_1T + a_2T^2)\ \ln\left[\frac{N}{N_o(1 + b_1T)}\right] \qquad \text{(B5)}$$

where $T(\geq$ 300 K) is the temperature, the parameters a_o, and N_o are the gain coefficient and carrier concentration at transparency. In (B5), a_o and N_o are assumed to be varied with L_d and their dependences with L_d are given in Table II. The temperature dependence of G is approximated by the coefficients $a_1 = 3.0815 \times 10^{-3}$ K^{-1}, $a_2 = 5.316\,95 \times 10^{-6}$ K^{-2}, and $b_1 = 6.017 \times 10^{-3}$ K^{-1}. However for $L_d > 20$ Å, the TE optical gain, G, at 0.85 μm is approximated by a linear relation and is given as

$$G = a_g(N - N_g) \qquad \text{(B6)}$$

where a_g and N_g are the fitted parameters and are assumed to be varied with $L_d > 20$ Å only. The values of these parameters are given in Table III. The temperature dependence of G with $L_d > 20$ Å is ignored in our calculation because the change of optical loss with operation wavelength is almost negligible (i.e., shift of gain spectrum due to temperature effect) [see Fig. 2(b)].

The carrier-induced refractive index change, Δn, which varies with the background refractive index profile of the active region, can be obtained from the change of the gain coefficient, $\Delta G(\omega) = G(\omega)$–$G_o(\omega)$, through the Kramers–Kronig dispersion relation [13]

$$\Delta n(\omega) = \frac{\pi}{c}\,\mathrm{PV}\int_0^{\infty}\frac{\Delta G(\omega')}{\omega'^2 - \omega^2}\,d\omega' \qquad \text{(B7)}$$

where $G_o(\omega)$ is the optical gain at transparency. The symbol PV stands for the Cauchy principle value. We can also approximate the carrier-induced refractive index change, Δn, at 0.85 μm with L_d varying between 0 and 20 Å by the following expression:

$$\Delta n = d_0(1 + d_1T + d_2T^2)\ \ln\left[\frac{N}{N_r(1 + e_1T)}\right] \qquad \text{(B8)}$$

where the parameters d_o and N_r are assumed to be varied with L_d only. Their dependencies on L_d are also given in Table II. The temperature dependence of Δn is approximated by the coefficients $d_1 = 2.0791 \times 10^{-4}$ K^{-1}, $d_2 = 1.3658 \times 10^{-7}$ K^{-2}, and $e_1 = 3.62 \times 10^{-2}$ K^{-1}. However for $L_d > 20$ Å, the refractive index change due to the injection carrier concentration and the variation of temperature are ignored in our calculation for the same reason as discussed before.

APPENDIX C

Fig. 7 shows the periodic DFQW structure of the semiconductor FP laser. The period of the periodic DFQW structure consists of two sections: a gain section (G) with $L_d = 0$ Å and a loss section (L) with $L_d = 5$–100 Å. The sequence of the gain/loss section of the periodic DFQW structure is assumed to be $G, L, \cdots, G, L, G, G, L, G, \cdots, L, G$. The neighboring gain sections in the device center are used to provide a $\lambda/4$ phase-shifted for the excitation of the gap mode. The gain/loss section of the periodic DFQW structure can be represented by a scattering matrix, M_k, which is given (C1), shown at the bottom of the page [17], where k is the section number, ne is the effective refractive index, $\gamma_k = j\beta_k - g_k/2$, β_k ($= 2\pi ne_k/\lambda_o$) is the propagation constant, and g_k ($= \Gamma_k G_k - \alpha_s$) is the net power gain of the kth diffused section. Δz_k in (C1) is the longitudinal length of the diffused sections. The spontaneous emission is exploited in the center of the laser (see Fig. 7) so that the longitudinal propagating fields, F and R, can be solved in a matrix format [18] as follows:

$$\begin{aligned}\begin{bmatrix}F_n'\\ R_n'\end{bmatrix} &= \prod_{k=1}^{N_d}[M_k]\begin{bmatrix}F_1\\ R_1\end{bmatrix} + \prod_{k=1}^{N_d/2}[M_k]\begin{bmatrix}I_f\\ I_r\end{bmatrix}\\ &= \begin{bmatrix}T_{11} & T_{12}\\ T_{21} & T_{22}\end{bmatrix}\begin{bmatrix}F_1\\ R_1\end{bmatrix} + \begin{bmatrix}S_{11} & S_{12}\\ S_{21} & S_{22}\end{bmatrix}\begin{bmatrix}I_f\\ I_r\end{bmatrix}\end{aligned} \qquad \text{(C2)}$$

$$M_k = \begin{cases}\dfrac{1}{2ne_{k+1}}\begin{bmatrix}ne_k + ne_{k+1} & ne_k - ne_{k+1}\\ ne_k - ne_{k+1} & ne_{k+1} + ne_k\end{bmatrix}\begin{bmatrix}e^{-\gamma_k\Delta z_k} & 0\\ 0 & e^{\gamma_k\Delta z_k}\end{bmatrix} & 1 \leq k < N_d\\ \begin{bmatrix}e^{-\gamma_k\Delta z_k} & 0\\ 0 & e^{\gamma_k\Delta z_k}\end{bmatrix} & k = N_d\end{cases} \qquad \text{(C1)}$$

where I_f and I_r are the spontaneous emission noise coupled into the forward and reverse fields. The lasing conditions for the longitudinal modes can be evaluated from the boundary conditions at the laser facets

$$F_1 = r_L R_1$$

and

$$R'_n = r_R F'_n \tag{C3}$$

where r_L and r_R are the left and right facet reflectivities, respectively. By substituting (C3) into (C2), we get

$$\begin{bmatrix} r_L R_1 \\ R_1 \end{bmatrix} = \begin{bmatrix} 0 & 0 \\ r_L & 1 \end{bmatrix} \begin{bmatrix} 1 & -r_L T_{11} - T_{12} \\ r_R & -r_L T_{21} - T_{22} \end{bmatrix}^{-1} \cdot \begin{bmatrix} S_{11} & S_{12} \\ S_{21} & S_{22} \end{bmatrix} \begin{bmatrix} I_f \\ I_r \end{bmatrix} \tag{C4}$$

and the average photon density, P, output from the left facet is given by

$$P = [r_L^* R_1^* \quad R_1^*] \begin{bmatrix} r_L R_1 \\ R_1 \end{bmatrix} \tag{C5}$$

where we have assumed $I_f I_f^* = I_r I_r^* = \nu_g B_{sp} \overline{N}^2 / \Delta z$ and $\overline{N}$ is the average carrier concentration.

ACKNOWLEDGMENT

The authors would like to thank Dr. P. Shum of the Department of Electrical and Electronic Engineering, Hong Kong University, Hong Kong, or his careful reading of this manuscript.

REFERENCES

[1] J. S. Major, S. O'Brien, V. Gulgazov, D. F. Welch, and R. J. Lang, "High-power single-mode AlGaAs distributed Bragg reflector laser diodes operating at 856 nm," *Electron. Lett.*, vol. 30, pp. 496–497, 1994.

[2] H. Soda, Y. Kotaki, H. Sudo, H. Ishikawa, S. Yamakoshi, and H. Imai, "Stability in single longitudinal mode operation in GaInAsP/InP phase-adjusted DFB lasers," *IEEE J. Quantum Electron.*, vol. QE-23, pp. 804–814, 1987.

[3] J. E. A. Whiteaway, G. H. B. Thompson, A. J. Collar, and C. J. Armistead, "The design and assessment of $\lambda/4$ phase-shifted DFB laser structure," *IEEE J. Quantum Electron.*, vol. 25, pp. 1261–1279, 1989.

[4] H. Hillmer, K. Magari, and Y. Suzuki, "Chirped gratings for DFB laser diodes using bent waveguides," *IEEE Photon. Technol. Lett.*, vol. 5, pp. 10–12, 1993.

[5] P. Zhou and G. S. Lee, "Chirped grating $\lambda/4$ shifted DFB laser with uniform longitudinal field distribution," *Electron. Lett.*, vol. 26, pp. 1660–1661, 1990.

[6] J. Salzman, H. Olesen, A. Møller-Larsen, O. Albrektsen, J. Hanberg, J. Nørregaard, B. Jonsson, and B. Tromborg, "Distributed feedback lasers with an S-bent waveguide for high power single mode operation," *IEEE J. Select. Topics Quantum Electron.*, vol. 1, pp. 346–355, 1996.

[7] S. Hansmann, H. Hillmer, H. Walter, H. Burkhard, B. Hubner, and E. Kuphal, "Variation of coupled coefficients by sampled gratings in complex coupled distributed feedback lasers," *IEEE J. Select. Topics Quantum Electron.*, vol. 1, pp. 341–345, 1996.

[8] G. P. Agrawal and N. K. Dutta, *Long-Wavelength Semiconductor Lasers.* New York: Van Nostrand Reinhold, 1986.

[9] C. C. Lee and D. H. Chien, "The effect of bonding wires on longitudinal temperature profiles of laser diode," *J. Lightwave Technol.*, vol. 30, vol. 14, pp. 1847–1852, 1996.

[10] J. Kinoshita, K. Ohtsuka, H. Agatsuma, A. Tanaka, T. Matsuyama, A. Makuta, and H. Kobayashi, "Performance of 1.5μm DFB lasers with a narrow stripe region," *IEEE J. Quantum Electron.*, vol. 27, pp. 1759–1765, 1991.

[11] L. M. Zhang, S. F. Yu, M. C. Nowell, D. D. Marcenac, J. E. Carroll, and R. G. S. Plumb, "Dynamic analysis of radiation and side-mode suppression in a second-order DFB laser using time domain large signal travelling wave model," *IEEE J. Quantum Electron.*, vol. 30, pp. 1389–1395, 1994.

[12] E. H. Li, B. L. Weiss, K. S. Chan, and J. Micallef, "The polarization dependent refractive index of an interdiffusion induced AlGaAs/GaAs quantum well," *Appl. Phys. Lett.*, vol. 62, pp. 550–552, 1992.

[13] C. H. Herny, R. A. Logan, and K. A. Bertness, "Spectral dependence of the change in refractive index due to carrier injection in GaAs lasers," *J. Appl. Phys.*, vol. 52, pp. 4457–4461, 1981.

[14] E. H. Li and K. S. Chan, "Laser gain and current density in a disordered AlGaAs/GaAs quantum well," *Electron. Lett.*, vol. 29, pp. 1233–1234, 1993.

[15] W. P. Gillin, I. V. Bradley, L. K. Howard, R. Gwilliam, and K. P. Homewood, "The effects of silicon and beryllium on the interdiffusion of GaAs/Al$_x$Ga$_{1-x}$As/GaAs quantum well structures," *J. Appl. Phys.*, vol. 73, no. 11, pp. 7715–7719, 1993.

[16] R. F. Kazarinov and C. H. Henry, "Second-order distributed feedback lasers with mode selection provided by first-order radiation loss," *IEEE J. Quantum Electron.*, vol. QE-21, pp. 144–150, 1985.

[17] E. Hecht, *Optics.* Boston, MA: Addison-Wesley, 1974, ch. 4.

[18] L. M. Zhang and J. E. Carroll, "Large signal dynamic model of the DFB lasers," *IEEE Quantum Electron.*, vol. 28, pp. 604–611, 1992.

[19] S. R. Andrew, J. H. Marsh, M. C. Holland, and A. H. Kean, "Quantum well laser with integrated passive waveguide fabrication by neutral impurity disordering," *IEEE Photon. Technol. Lett.*, vol. 4, pp. 426–428, 1992.

[20] C. Kaden, H. Grabeldinger, H. P. Gauggel, V. Hofsaβ, A. Hase, A. Menschig, H. Schweizer, R. Zengerle, and H. J. Bruckner, *Microelectron. Eng.*, vol. 23, p. 469, 1994.

[21] S. F. Yu and E. H. Li, "Proposed enhancement of side mode suppression ratio in $\lambda/4$ shifted distributed feedback lasers with nonuniform diffused quantum wells," *IEEE Photon. Technol. Lett.*, vol. 8, pp. 482–484, 1996.

[22] V. Hofsäß, J. Kuhn, C. Kaden, V. Härle, H. Bolay, F. Scholz, H. Schweizer, H. Hillmer, R. Lösch, and W. Schlapp, "Optical integration of laterally modified multiple quantum well structures by implantation enhanced intermixing to realize gain coupled DFB lasers," *Nucl. Instrum. Methods Phys. Res. B*, vol. 106, pp. 471–476, 1995.

[23] W. B. Joyce and R. W. Dixon, "Thermal resistance of heterstructure lasers," *J. Appl. Phys.*, vol. 46, pp. 855–862, 1975.

[24] R. S. Zory, Ed. *Quantum Well Lasers.* New York: Academic, 1993, ch. 1.

S. F. Yu received the B.Eng. degree (with Departmental Prize) in electronic engineering from London University, University College, England, in 1990 and the Ph.D. degree in optoelectronics from Cambridge University, Robinson College, England, in1993.

He joined the Department of Electronic Engineering, Sha Tin Technical Institute, Hong Kong, as a part-time lecturer in 1993. In 1994, he joined the Department of Electrical and Electronic Engineering, the University of Hong Kong, Hong Kong, where he was a Lecturer. since 1996, he has been an Assistant Professor in the same department. His main research topics include wavelength selectivity of grating coupled waveguides, transient properties of semiconductor laser diodes, and design of optoelectronics integrated circuit. He currently conducts the development of high-performance semiconductor lasers using diffused quantum-well material for the application in high-speed communication systems. He is also involved in the investigation of optical soliton fiber communication systems. He has published over 40 technical papers and one book chapter.

Dr. Yu is a Fellow and Honorary Scholar of the Cambridge Commonwealth Trust Society. He held a Croucher Foundation scholarship and an overseas research student award while completing the doctoral program. His biography is published in the fourth edition of *Who's Who in Science and Engineering*, the 25th edition of *The Dictionary of International Biographies*, an the 17th edition of *The International Directory of Distinguished Leadership*. For further information, contact the personal home page at http://www.eee.hku.hk/˜sfyu.

C. W. Lo was born in Hong Kong on October 29, 1971. He received the B.Sc. (Honors) degree in physics from the University of Hong Kong in 1994. He is currently working towards the M.Phil. degree at the same institution and will be graduating this year. His thesis is titled "Improvement of Semiconductor Laser Diodes' Characteristics by Using Diffused Quantum Wells Structure."

His research interest are concerned with the development of high-performance semiconductor lasers (including Fabry–Perot, distributed feedback, and vertical-cavity surface-emitting types) using diffused quantum-well structure. The influence of spatial hole burning of carrier concentration, thermal effects, carrier transport, waveguide dimension, and other nonlinear optical properties of semiconductor lasers are also considered in the investigation. He has published six technical papers and one book chapter while pursuing the M.Phil degree.

E. Herbert Li (S'87–M'88–SM'95) received the M.Phil. degree in applied mathematics and electronic engineering from the University of Hong Kong and the Ph.D. degree in electronic engineering from the University of Surrey, U.K.

He worked for the Kirsten Aeronautical Laboratory, Seattle, WA (1979–1980). He joined K K Engineering Co., Hong Kong, as an Engineer (1981–1986), and Micro Systems, Hong Kong, as a Manager (1986–1988). He was a Member of Faculty at the City University of Hong Kong (1988–1990). He joined the National Ion Implantation Facility at the Department of Electrical and Electronic Engineering, University of Surrey (1990–1993). He is currently a Member of Faculty and Leader of the Optoelectronics Group, which consists of a team of 10 researchers, at the Department of Electrical and Electronic Engineering, University of Hong Kong (1994–present). He is an Adjunct Professor of the Institute of Semiconductors, Shandong Normal University, China, and a Visiting Faculty Member at the University of Waterloo, Canada. His current research interests are mainly concerned with optoelectronic device fabrication, modeling and characterization, and in particular interdiffusion induced modification of quantum-well structures for the advanced performance and integration of optoelectronic devices. Since 1990, he has published over 100 international technical papers, two book chapters, and three books in the above area. He serves on both the Technical Program and International Advisory Committees of OECC in 1996 (Japan) and 1997 (Korea). He is an Editor of the *International Journal of Optoelectronics.*

Dr. Li is a "Distinguished Lecturer" of IEEE-EDS for 1997, and he is an AdCom *ex officio* member and EDS Meeting Committee member of the IEEE. He received the J. Langham Thompson Premium Prize in 1992 from the Institution of Electrical Engineers (U.K.) and the Distinguished Pioneering Projects Award in 1989 from HKCSS (Hong Kong). His biography is published in *Who's Who in Science and Engineering.*